

Advancing physics-based ground motion modelling of  
the 2016 Kaikoura Earthquake: Modelling basin-edge  
effects in Wellington and implications for seismic  
design  
Final Report

Brendon A. Bradley<sup>1</sup>, Robin L. Lee<sup>1</sup>, Liam Wotherspoon<sup>2</sup>, and Robert  
Graves<sup>3</sup>

<sup>1</sup>Department of Civil and Natural Resources Engineering, University of  
Canterbury, New Zealand

<sup>1</sup>Department of Civil and Environmental Engineering, University of  
Auckland, New Zealand

<sup>1</sup>USGS, Pasadena

2 February 2021

# 1 Executive Summary

Ground motions in the Wellington region observed during the 2016 Kaikura earthquake exhibited appreciable amplitudes at long vibrations periods ( $T > 1$  s) that resulted in relatively larger demands to multi-storey structures and consequent damage. Preliminary research by the authors and others has already illustrated that site amplification in the Wellington CBD region has occurred in past events - in particular, the 2013 Seddon and Lake Grassmere events, and therefore can be inferred to occur in future events also.

This report documents further research that has been undertaken to examine the systematic site effects (including so-called ‘basin-effects’) that exist in Wellington city as observed through ground-motion observations in multiple historical earthquakes, as well as informed through ground-motion simulations. In particular, 19 historical earthquakes above  $M = 5$  in the Wellington region were used to understand systematic site amplification relative to a nearby reference station. It is illustrated that the amplifications consistently exceed those prescribed through the use of NZS1170.5 (code-based) site amplification factors - implying that the seismic hazard at these locations (all other things equal) is underestimated.

A second approach, examining the systematic difference between observed and predicted ground motions from empirical ground-motion models (GMMs), was used to construct non-ergodic site amplification factors which can be used in so-called non-ergodic probabilistic seismic hazard analysis. It is illustrated that at moderate-to-long vibration periods, both the ‘reference site’ and ‘non-ergodic’ site amplification approaches yield similar results.

Finally, the empirically observed results from ground-motion observations are used to examine the predictive capability of physics-based ground motion simulations with a preliminary version of a Wellington sedimentary basin model. It is illustrated that the simulations capture the basic features of basin amplification, however further fine-tuning is needed to capture the spatial variation in ground motion. These simulations highlight a hypothesis that the depth of sedimentary material overlying basement rock (including highly weathered material) is deeper than current inferences; and further illustrate the need for non-invasive and invasive data collection to provide improved constraint on the basin geometry and geophysical properties.

## 2 Technical Abstract

This report addresses three approaches to examine so-called ‘basin-effects’ that result in stronger-than-expected ground motion amplitudes at moderate-to-long vibration periods in Wellington region. Two of the approaches make direct use of observed ground motions to develop empirical models, while a third approach uses numerical simulations that are subsequently compared with data. The results of these approaches highlight:

1. Site amplification predicted using the NZS1170.5 (code-based) prescriptions underestimates the level of amplification that is systematically observed in 19 historical earthquakes above magnitude 5;
2. Two empirical approaches for estimating systematic site effects yield consistent results at moderate-to-long vibrations periods, and these form a basis for the development of short-term empirical adjustments to seismic hazard analysis results for the Wellington city region to account for such effects;
3. Ground-motion simulations provide significant potential to treat basin-effects in a holistic manner in Wellington (as well as other NZ locations), and are able to capture the essential features of basin amplifications, but would benefit significantly by additional data collection to constrain the geometry and geophysical properties of the Wellington basin.

# Contents

<b>1 Executive Summary</b>	<b>2</b>
<b>2 Technical Abstract</b>	<b>3</b>
<b>3 Observations of site and basin amplification in the Wellington region</b>	<b>5</b>
<b>4 Improved seismic site characterisation</b>	<b>7</b>
4.1 Deep characterisation of Wellington's CentrePort . . . . .	7
4.2 Wellington basement depth map . . . . .	7
<b>5 Quantification of basin amplification: Empirical modelling</b>	<b>8</b>
5.1 Earthquakes and sites considered . . . . .	8
5.2 Method 1: Direct site amplification . . . . .	10
5.2.1 Theory . . . . .	10
5.2.2 Results . . . . .	10
5.3 Method 2: Mixed-effects analysis . . . . .	12
5.3.1 Theory . . . . .	12
5.3.2 Results . . . . .	13
5.4 Comparison of methods and recommendation . . . . .	14
5.5 Discussion and limitations . . . . .	14
5.5.1 Applicability for use with various empirical models . . . . .	15
5.5.2 Physical parameters that are represented in the amplification factors	15
<b>6 Quantification of basin amplification: Simulation modelling</b>	<b>15</b>
6.1 Summary . . . . .	15
6.2 Wellington velocity model . . . . .	16
6.3 Spectral ratios from simulations . . . . .	16
6.4 Sensitivity study . . . . .	16
6.4.1 3D simulations: Minimum $V_s = 300m/s$ sensitivity study . . . . .	16
6.4.2 3D simulations: Weathered basement sensitivity study . . . . .	17
6.5 2D simulations . . . . .	17
6.6 Summary insights from preliminary simulation work . . . . .	17
<b>7 Ongoing work required</b>	<b>17</b>
<b>8 Acknowledgements</b>	<b>18</b>

### 3 Observations of site and basin amplification in the Wellington region

Figure 1 illustrates the location of Wellington city in the context of the 2016 Kaikura and 2013 Seddon and Lake Grassmere earthquakes. Additionally, Figure 1c also illustrates the surficial geology and location of strong-motion stations that recorded ground motions during these earthquake, among others.

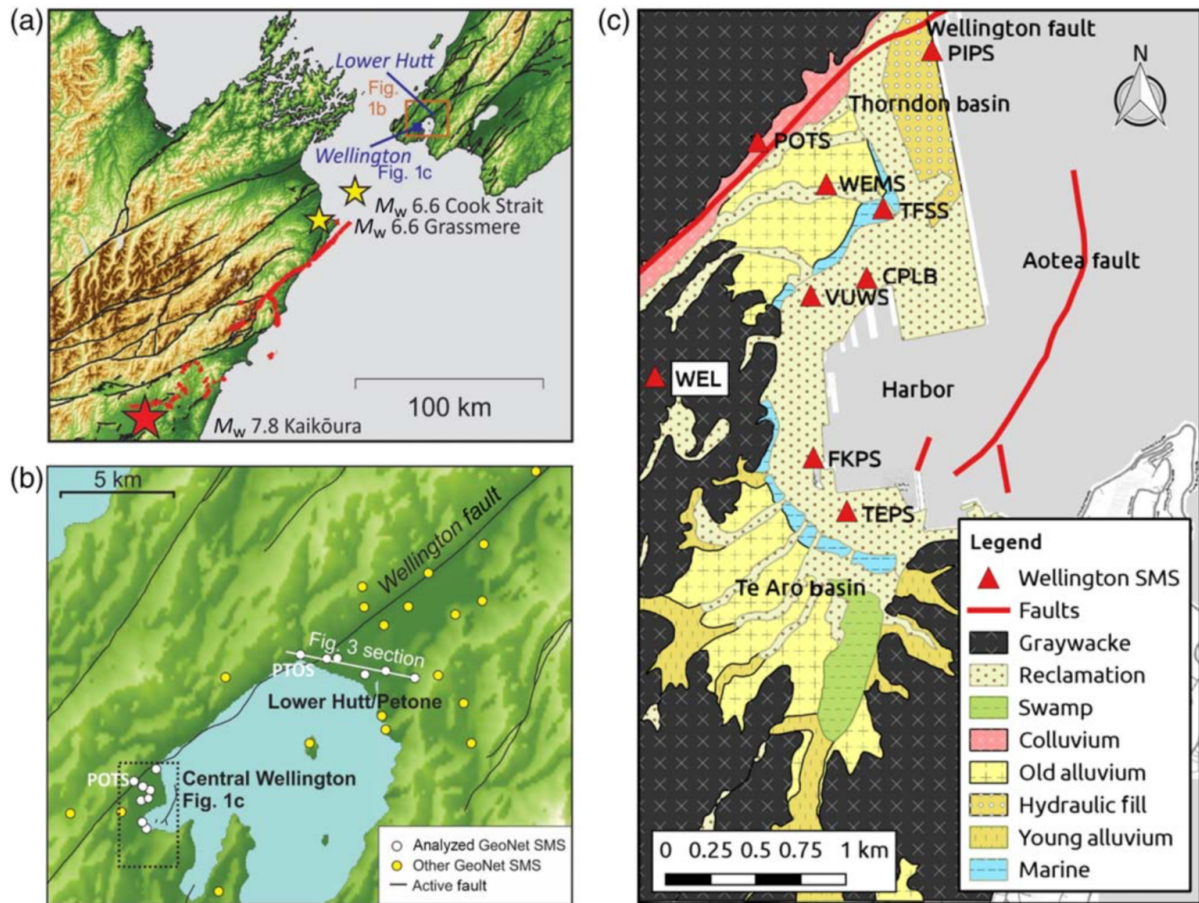


Figure 1: Regional context for Wellington city's ground-motion observation locations in the context of the 2016 Kaikura and 2013 Seddon and Lake Grassmere earthquakes. After Bradley et al. [2018].

The wide appreciation for the need to understand the site-specific amplification of ground motions in Wellington city is the observations of large ground motions in the 2016 Kaikura earthquake. Figure 2 illustrates the horizontal and vertical response spectra observed at the locations noted in Figure 1c. The horizontal spectra of sites in the Thorndon and Te Aro basins are seen to exhibit appreciable amplifications relative to those of rock sites, such as POTS illustrated in the figure. The vertical ground motions in the Thorndon basin, in particular, also exhibit appreciable amplification in the vertical component - which indicate the significant presence of basin-generate Rayleigh waves [Bradley et al., 2017c].

Such amplifications at soil sites are not unique to the 2016 Kaikura earthquake. Bradley et al. [2017c] and Bradley et al. [2018] illustrate that such effects are also observed

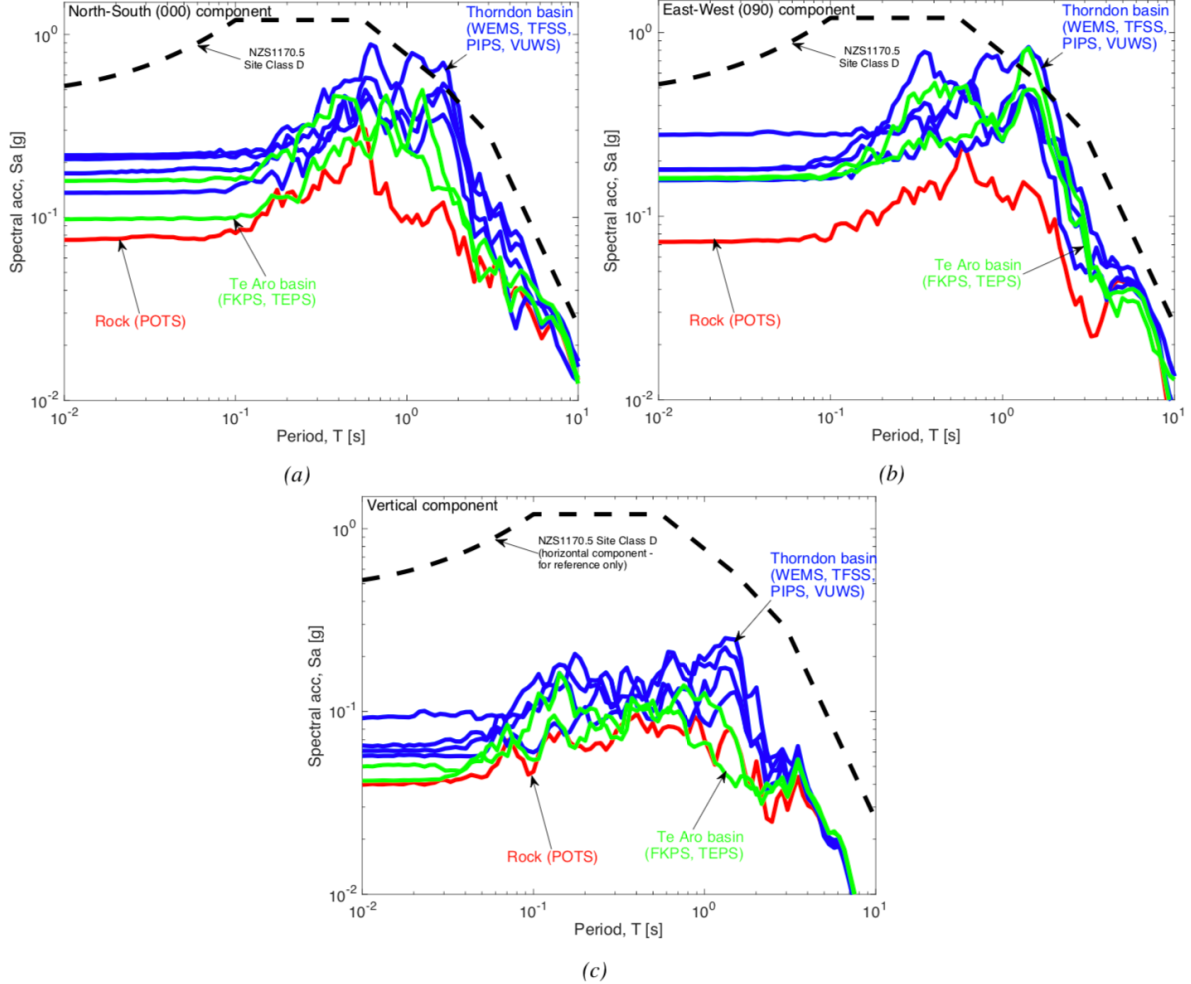


Figure 2: Comparison of response spectra in three orthogonal components: (a) North-south (000); (b) East-west (090); and (c) vertical segregated by basin location or rock. After Bradley et al. [2017c].

in the 2013 Seddon and Lake Grassmere earthquakes, therefore implying that such effects are systematic, and can be expected to also occur in future events.

As well as these effects being apparently systematic, Bradley et al. [2017c] illustrate that the degree of site amplifications are consistently larger than those prescribed by seismic design standards for a wide range of vibration periods. Figure 3 illustrates that over the vibration period range of  $T=1\text{-}2$  s mean amplifications in Wellington soil sites are approximately 3.0 - well above the prescribed amplifications for Site Class C and D sites.

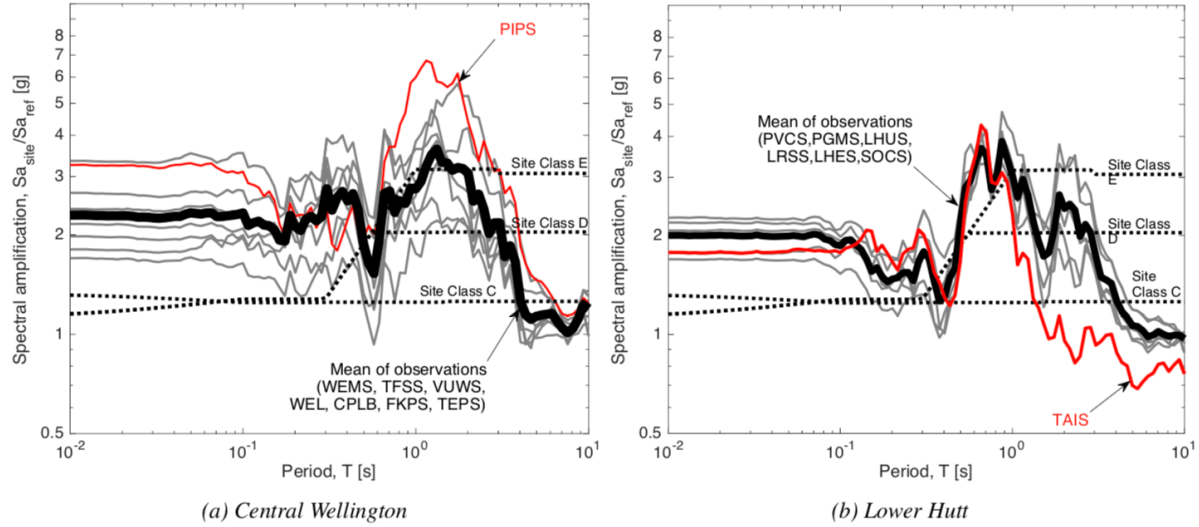


Figure 3: Spectral amplifications of soil stations in: (a) Wellington with reference to the POTS rock station; and (b) Lower Hutt with reference to the PTOS rock station. PIPS and TAIS stations are specifically identified for reasons noted in the text. The mean of the remaining six stations is also shown. After Bradley et al. [2017c].

## 4 Improved seismic site characterisation

Several avenues to improve the characterisation of the shallow and deep sediments in the Wellington basin were undertaken with partial funding from this project. Both are published in separate documents, so are only briefly summarised here.

### 4.1 Deep characterisation of Wellington's CentrePort

CentrePort resides on some of the deepest sediments in the Wellington CBD region and therefore is an ideal test location for examining basin depth properties. Figure 4 illustrates the locations where surface wave testing was performed, as discussed further in Vantassel et al. [2018], and used to obtain estimates of site period (as shown), as well as the underlying velocity profiles with depth. The inferred depths to basement rock were shallower than those of Semmens et al. [2011].

### 4.2 Wellington basement depth map

The results of the above surface wave testing fed into an update of the Wellington basement depth model of Kaiser et al. [2019], with the input of project member Liam Wotherspoon. Figure 5 provides a comparison of the original basin depth map used in Semmens et al. [2011] with that of Kaiser et al. [2019]. This updated basin depth map was developed late in the timeline of this present project, therefore the simulations performed utilized the prior Semmens et al. [2011] model, and hence the potential for further work to examine the impacts of this more recent revision.

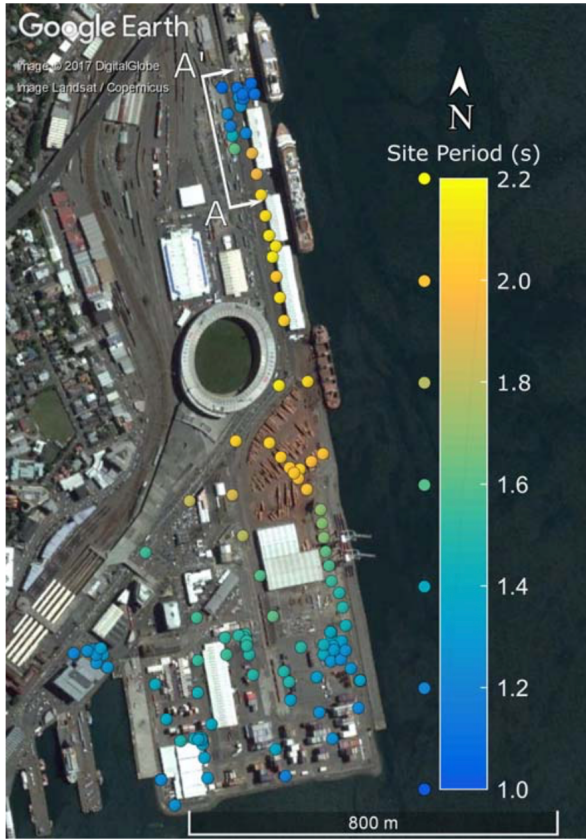


Figure 4: Test locations in CentrePort where non-invasive surface wave data was collected to infer site period and velocity profiles.

## 5 Quantification of basin amplification: Empirical modelling

### 5.1 Earthquakes and sites considered

Two datasets of historical earthquakes are considered, which are illustrated in Figure 6. The dataset used in Method 1 is based on 19 events with  $M_w \geq 5$ , and for method 2 based on 195 events with  $M_w \geq 3.5$ . The reason for using two different datasets was to leverage on-going research results performed by University of Canterbury researchers - which are adopting different datasets for different reasons. The smaller dataset focuses on the use of larger magnitude events (in a relative sense), and the second dataset focuses on a more comprehensive analysis and therefore makes use of additional data. The subsequent results illustrate that consistent results are obtained.

In Method 1 (details subsequently presented), the analyses are performed on a station-by-station basis (i.e. there is no dependence of the observed ground motions at station X and station Y). In contrast, in Method 2, there is a dependence on the results depending on the stations considered. As a consequence, in Method 1 only stations of interest (in Wellington city) are considered, whereas in Method 2 a larger number of stations across the entire Wellington region are considered (in order to ensure that any local effects are averaged-out by considering a wide region). This can be seen by the significantly larger number of stations (blue triangles) in Figure 6b relative to Figure 6a.

Figure 1c illustrates the location of the strong motion stations (that are discussed

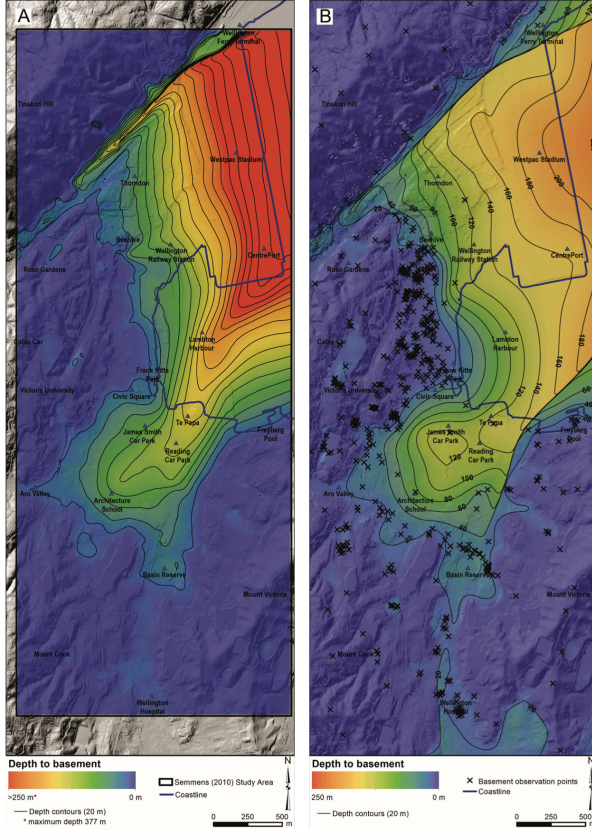


Figure 5: Comparison of depth to basement of Semmens et al (left) and updated Kaiser et al. models. After Kaiser et al. [2019].

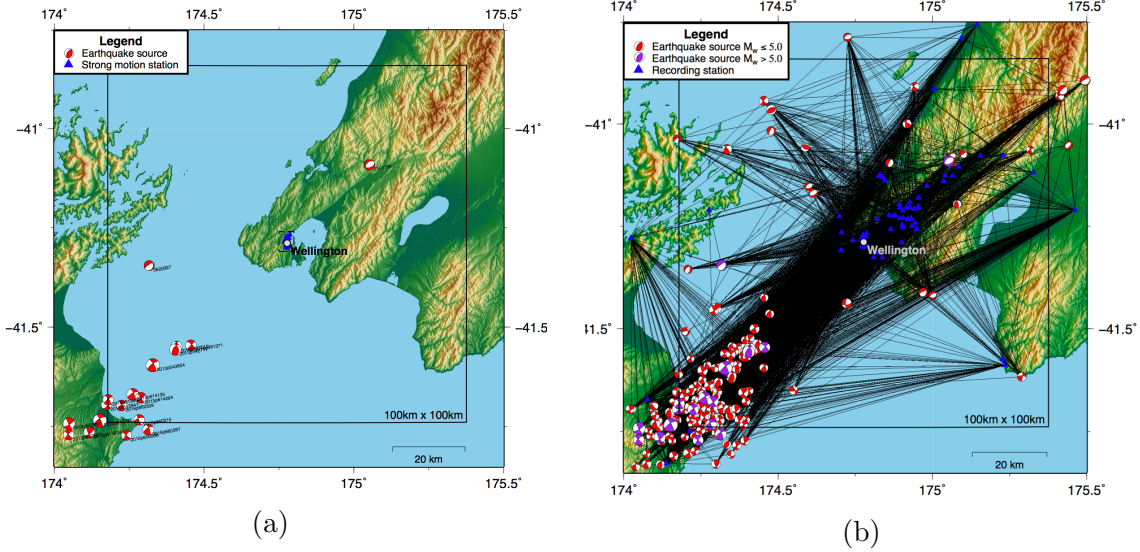


Figure 6: (a) Geographical location of 19  $M_w \geq 5$  earthquakes and the considered strong motion stations in the urban Wellington region used in Method 1; and (b) location of the 195  $M_w \geq 3.5$  earthquakes and considered strong motion stations in Method 2.

to varying degrees in subsequent sections) considered to empirically examine seismic site effects in the Wellington city area. They can be grouped into those located in the Thorndon and Te Aro basins, as shown in the figure. Evidence presented by Bradley et al.

[2017c, 2018] indicates that there is a notable difference between the two different basin response, and attention is given to the Thorndon basin response. Bradley et al. [2017c, 2018], and the subsequently presented analysis results, also illustrate that the observed ground motions at the WEMS site deviate from the remaining three Thorndon basin sites (VUWS, TFSS, PIPS) - and hence attention is principally given to these three sites.

One clear area of uncertainty throughout this report is the assumption as to what site effects at a general location in Thorndon relative to those at the specific strong-motion station locations. To illustrate the general method, the average of observed results is taken, though for site-specific implementation a non-uniform weighting of observations is possible based on spatial considerations. Specifically, the subsequent results indicate that the PIPS site exhibits larger long period ground motion amplification than the other two sites. Such amplitudes may be specific to the region near the PIPS site (Aotea Quay) because of its close proximity to the Wellington fault<sup>1</sup>. Clearly the most prudent approach would be to install instruments at other locations over the Thorndon basin region in order to be able to have a data-driven understanding of site amplification.

Finally, the subsequently presented results using Method 2 require the explicit consideration of the  $V_{30}$  values of the strong motion stations. For this the compiled data of Kaiser et al. [2017] was adopted. It is noted that the values for the three sites of primary interest are:  $VUWS = 250 \text{ m/s}$ ;  $TFSS = 274 \text{ m/s}$ ; and  $PIPS = 210 \text{ m/s}$ . The average of these three is  $244.7 \text{ m/s}$ .

## 5.2 Method 1: Direct site amplification

### 5.2.1 Theory

Earthquake-induced ground motions can be considered as a function of source, path and site effects. In order to isolate the surficial site effect, recorded ground motion intensities are normalized by the intensities that are observed at a nearby reference rock site. Because of their adoption in seismic design and assessment, we utilize response spectra to quantify the site amplification.

Mathematically, the site amplification is obtained from the spectral ratio of the soil and reference rock site as:

$$Amp_i(T) = \frac{SA_i(T)}{SA_{rock}(T)} \quad (1)$$

where  $T$  is the response spectral period;  $SA_i$  and  $SA_{rock}$  are the (pseudo) spectral acceleration at soil site  $i$  and reference rock site, respectively. Each of the 19 events is considered as equally representative of the soil amplification for the purpose of computing mean amplifications over the ensemble of events (although we do also explicitly examine the effect of nonlinearities on the observed amplifications).

### 5.2.2 Results

**Observations and comparison to code-based amplifications** Figure 8 illustrates the spectral amplifications several example sites. Figures 8a-d are for sites in the Thorndon basin, while Figures 8e-f are for sites in the Te Aro basin. For each figure panel, as well as the individual spectral amplifications for the 19 events, the mean amplification across all events, the specific amplification for the 2016 Kaikoura earthquake, and the

---

<sup>1</sup>and thus lateral velocity variation in the subsurface across the fault that can lead to large basin wave generation

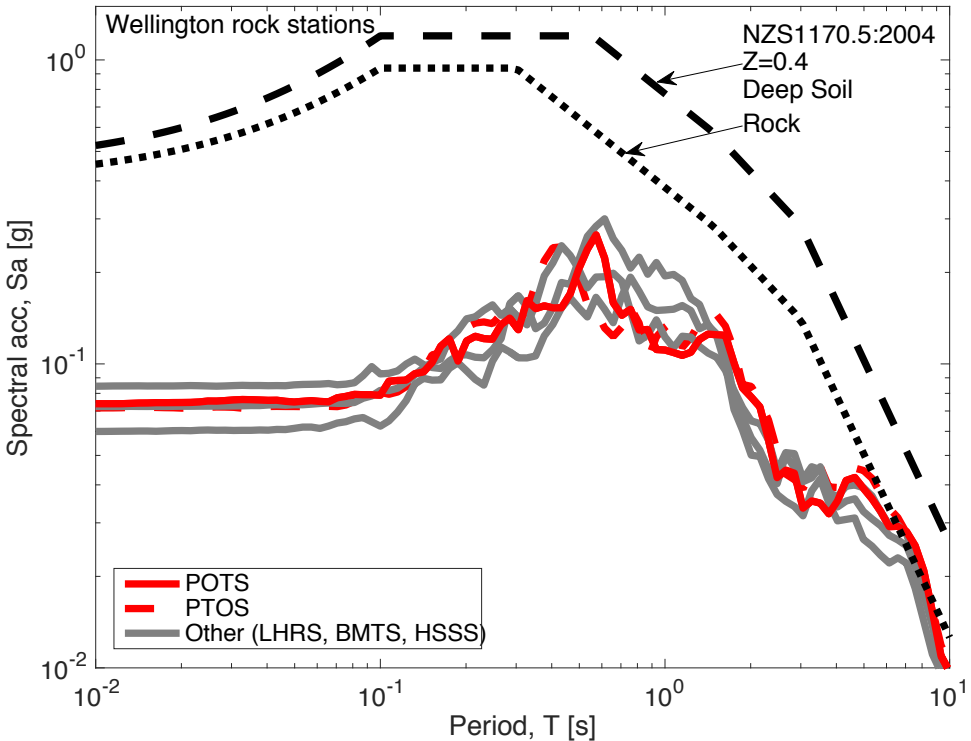


Figure 7: Response spectra of observed ground motions at rock stations during the 14 November 2016 Kaikoura earthquake (after Bradley et al. [2017b]).

NZS1170.5:2004 site class D site amplification are also provided. To clarify, firstly, the 2016 Kaikoura spectral amplification is specifically annotated because it is valuable to appreciate the amplification in this largest ground motion amplitude case relative to mean of the 19 events, which are predominantly smaller in amplitude. Secondly, the site class D spectra is provided in all cases because the majority of the sites would be classified as site class D according to NZS1170.5:2004 and thus that code-based site amplification serves as a design reference versus that which is actually occurring.

In Figure 8 it can be seen that PIPS, WEMS, and TFSS sites (in Thorndon basin) have appreciable amplification over the range  $T = 0.5 - 5.0\text{s}$  relative to implied site class D spectra. The TEPS site (in Te Aro basin) also exhibits significant amplification over the  $T = 0.5 - 5.0\text{s}$  period band, but principally over the  $T = 0.5 - 2.0\text{s}$  range. The remaining two stations, VUWS and FKPS, also exhibit mean amplifications that exceed the code-based amplifications over this period range, although not as spectacularly. Importantly, across the 19 individual events considered, there is a very consistent level of amplification observed at each site (as indicated by their corresponding mean amplification).

Comparing the mean amplification from 19 events with the amplification specifically in the 2016 Kaikoura earthquake also illustrates that they are generally similar. The only notable exceptions to this is over the period range  $T = 0.5 - 1.5\text{s}$  and  $T > 5\text{s}$  (both approximate ranges). The former is inferred as the result of nonlinear site behaviour leading to a small reduction in site amplification (which, as noted previously, is more significant at shorter periods). The reduced amplification for long periods ( $T > 5\text{s}$ ) in the Kaikoura event occur as a result of the magnitude dependence of the response spectrum-based site amplification, as a result of the link between Fourier spectra amplification and its convolution to response spectra [Bora et al., 2016].

**Mean reference site amplification vs. empirical amplification** The results shown in the previous section compared the reference site amplifications with respect to the code-based site amplification. While useful, in the consideration of site-specific PSHA it is of more direct interest to compare the reference site amplifications with respect to the empirically-predicted site amplifications - that is the empirically-predicted amplification between the soil site and the reference rock site. The reason for this is that it is the empirical site amplification that is already used in the ergodic PSHA calculations, and therefore the aim is to understand how observations of site amplification may deviate from those empirically predicted.

Figure 9 provides a comparison between the mean spectral amplifications from Figure 8 and an empirically-predicted site amplification. The empirical site amplification is based on the use of a soil site with  $V_{s30} = 240m/s$  (which is representative of the strong motion station soil sites in Wellington), and  $V_{s30} = 1000m/s$  for the rock site (which is based on the  $V_{s30}$  value of POTS used in Kaiser et al. [2017]). Relative to the amplification factors based on NZS1170.5 (in Figure 8) it can be seen that empirically-predicted amplifications at long periods at larger (values on the order of 3.0, as compared to 2.0 for NZS1170.5 site class D), and also that the amplification decreases for very long periods (i.e. approaching  $T = 10s$ ). Strictly speaking, site amplification in empirical ground motion models is dependent on the amplitude of the ground motion used. In the result shown here, the intensity of the input ground motion is based on a  $M_w6.5$  earthquake at a distance of 30km, which yields relatively small ground motion intensities, and therefore the empirical result has little (but still some) influence of nonlinear effects. When the calculation is repeated using a magnitude distance combination that results in smaller ground motions (e.g.  $M_w5$  and  $R_{rup} = 100km$ ) then there is a minor change in the empirical amplification at short periods (from 1.3 up to 1.4) which decreases as the vibration period increases, and is practically identical for  $T > 1s$ . As a result, only one value of the empirical amplification is shown for simplicity, given the larger uncertainties in other assumptions.

Both of these differences between the empirical and code-based site prediction illustrate that the empirical amplification is more reflective of the observations. Despite these features of the empirical amplification relative to the code-based amplification, it can still be seen that in general the observed amplification are higher than those predicted empirically. Figure 10 illustrates the ratio of the reference site amplification and the empirically-predicted site amplification results in Figure 9. In addition to the results on a station-by-station basis, a model line is shown based on the mean of the three stations in Thorndon - VUWS, TFSS, and PIPS. The mean/model value in Figure 10 is approximately 2 at short periods and generally decreases with vibration period to be approximately 1 at long periods. Further discussion on the features of this figure are presented in Section 5.4.

## 5.3 Method 2: Mixed-effects analysis

### 5.3.1 Theory

The alternative to the reference site amplification via Method 1 is to make use of observations with respect to empirically-predicted ground motions, and determine systematic trends in the residual between observed and predicted. Mathematically, the observed ground motions can be expressed as:

$$\ln IM_{obs,e,s} = f_{IM,e,s} + a + \delta B_e + \delta S2S_s + \epsilon \quad (2)$$

where  $e$  and  $s$  represent indices for a specific earthquake event and site location, respectively; a  $\ln IM_{obs,e,s}$  is the (logarithm of the) observed intensity measure (for event  $e$  and site  $s$ );  $f_{IM}$  is the empirical (log median) prediction;  $a$  is the overall model bias (constant for all events and stations);  $\delta B_e$  is the between-event residual (varying between events, but a constant for all stations for a given event);  $\delta S2S_s$  is the between-site residual (varies by site, but constant for all events); and  $\epsilon$  is a ‘remaining’ residual to describe unaccounted deviations.

Other than the observed and median predicted values, all other terms in Equation 2 are determined by solving a mixed-effects regression. It is important to note that the terms  $a$  and  $\delta S2S_s$  are systematic at a given site; thus, by making use of systematic deviations as seen through observations it is possible to obtain an improved prediction as:

$$\ln IM_{obs,e,s} = (f_{IM,e,s} + a + \delta S2S_s) + \delta B_e + \epsilon \quad (3)$$

Alternatively, one can consider that the improved prediction is related to the original prediction via:

$$IM_{updated} = IM_{original} * \exp(a + \delta S2S_s) \quad (4)$$

where  $IM_{original} = \exp(f_{IM,e,s})$ .

### 5.3.2 Results

Using the 195 events and stations shown in Figure 6b, the mixed-effects analysis was performed according to Equation 2, and focus here is given to the systematic terms which influence the improved prediction as per Equation 4.

Figure 11a and b illustrate the bias,  $a$ , and site-term,  $\delta S2S_s$ , terms. The site terms are presented for the three stations that collectively encompass Thorndon basin - VUWS, TFSS, and PIPS (i.e. Figure 1c), and also for the POTS rock site.

Figure 11a illustrates that, overall, there is a minor bias in the empirical ground motion prediction across all of the sites, with a bias of approximately  $-0.2$  over the period range of  $T = 0.1 - 5.0s$ . For vibration periods  $T < 0.1s$  the bias increases in the negative sense. For vibrations periods  $T > 5.0s$  the bias begins to increase quite rapidly. Related to the long-period bias trend, it is well known that empirical ground motion models are less reliable at very long periods, and in particular the Bradley [2013] model under-predicts long period ground motions as noted in Van Houtte et al. [2017]. Because this is a problem with the Bradley et al. model alone (and not for other models used in the PSHA) then, for the purpose of the systematic correction factors herein, then the bias for  $T > 5s$  is set equal to the  $T = 5s$  value, as shown in the Figure.

Figure 11b illustrates that the three soils sites (VUWS, TFSS, PIPS) all have  $\delta S2S$  values that exceed zero. While there is variation amongst them, there is a general trend that makes the use of their mean (indicated by ‘Model’ line in grey) as indicative of the nominal site effects over the Thorndon basin in the absence of direct measurements. The  $\delta S2S$  term for the POTS rock station is also shown in the sense of additional insight into its use as a reference site for soil amplification (discussed below).

Figure 11c illustrates the systematic effect, i.e. Equation 4, which is the exponential of the summation of the results presented in Figure 11a and b. It can be seen that the mean (model) systematic effect for the soil sites is approximately 1 for  $T < 0.1s$ , increases to approximately 1.6 at  $T = 0.6s$  then decreases back to approximately 1 for  $T > 3s$ . The negative systematic term for POTS (for  $T < 0.2s$  and  $T > 2.0s$ ) indicates that the ground motions at this site are smaller than predicted empirically, with the under-prediction

at short periods being significant. There are several hypotheses for this, such as the POTS site may also have salient topographic deamplification or other effects that are not captured empirically. Most importantly, it is noted that if the POTS generally yields ‘smaller than expected’ ground motion amplitudes at short periods, then computing the spectral ratio with POTS on the denominator (i.e. Equation 1) means that the spectral ratio may be incorrectly large at short periods. Such factors should be borne in mind when examining the results of the reference site amplification results (i.e. Method 1).

## 5.4 Comparison of methods and recommendation

Figure 12 provides a direct comparison between the site amplification factors from Methods 1 and 2. For Method 1, this is the mean value of the site amplification after division by the empirically-predicted amplification (i.e. ‘Model’ presented in Figure 10). For Method 2, this is the mean value of the systematic effect presented in Figure 11c. It can be seen that the two results are similar for  $T > 0.2s$ , but diverge for  $T < 0.2s$ .

As noted in the discussion related to Figure 11c, it is inferred that the spectral ratio estimates for such short vibration periods computed using Method 1 are not robust because of the fact that the POTS site appears to record lower-than-expected ground motions at short periods. Because the POTS spectra are used in the denominator of Equation 1 for computing the spectral ratio, then lower POTS spectra at short periods suggest a higher site amplification. Here it should be kept in mind that the actual site amplification occurs between the surface and the rock directly beneath the surface - that is, the POTS rock site is being used as a surrogate for the rock underneath sites in the Thorndon basin because of the absence of direct recordings in the subsurface.

As a result of the acknowledged problems with Method 1 for short periods, it is proposed that the results of Method 2 are more robust for use in adjusting the ergodic PSHA results obtained from site-specific hazard analysis. In order to obtain smoothly-varying design response spectra, a smooth adjustment factor is proposed rather than using the direct results from Method 1. This smoothly-vary function is shown as ‘Proposed’ in Figure 12. It can be mathematically described by:

$$AF = \begin{cases} 1.0 & T \leq 0.1 \\ 1.0 + 0.6 \frac{\log(T/0.1)}{\log(0.6/0.1)} & 0.1 \leq T \leq 0.6 \\ 1.0 + 0.6 \frac{\log(3/T)}{\log(3/0.6)} & 0.6 \leq T \leq 3.0 \\ 1.0 & T \geq 3.0 \end{cases}$$

## 5.5 Discussion and limitations

The recommended approach to derive the site response amplification function presented in Figure 12 has been developed through the use of ground motion observations from historical events, at a specific set of site locations, and with reference to a single ground-motion model (in the case of the Method 2 results). In this vein there are several points worthy of discussion in the context of their use.

### **5.5.1 Applicability for use with various empirical models**

The amplification results from Method 2 are based on the use of a single empirical ground motion model, hence their use with other ground motion models (typically considered in a logic tree) is important. In this regard it is important to note that, via Equation 2 and 3, the residual between observation and empirical model prediction is partitioned into a total bias, between-event, between-site, and remaining residual terms. Because of the difference in the empirical model prediction, then the value of all of these terms is, strictly speaking, model dependent. However, the partitioning helps to significantly reduce the model dependence, specifically for the between-event and between-site terms. The general consistency of the results from Method 2 (using a single empirical model), with the results from Method 1 (which is based on a reference site approach, and thus does not require any empirical models) helps to empirically confirm this view.

### **5.5.2 Physical parameters that are represented in the amplification factors**

The proposed amplification factors represent the systematic difference between observed and empirically-predicted ground motions. As a result, they do not explicitly provide insight into the physical phenomena that are being captured. However, basic insight can be ascertained from other work which has examined the salient phenomena that have resulted in the observations. Examples include Bradley et al. [2017a,b]. Such research has indicated that appreciable basin-edge-induced surface waves are prevalent in the Thorndon basin region. Note that Bradley et al. [2017a] makes reference to basin amplification with respect to that prescribed in NZS1170.5:2004, whereas for this study it is with reference to the empirical ground motion models (used in the site-specific PSHA) that are of importance. As can be seen in Figure 9, the long period ground motion amplification within the empirical model (exceeding values of 3.0 at periods of approximately  $T = 1 - 5s$ ) is quite different to the amplification for the standard NZS1170.5:2004 site classes. Hence, it is the product of the 'Empirical GMM amplification' in Figure 9 and the proposed amplification function in Figure 12 that represent the site amplification relative to rock conditions. In this regard, the observations indicate that the generic empirical site amplification (Figure 9) is relatively adequate at long periods, but needs an increase over the  $T = 0.1 - 3s$  range, particularly around  $T = 0.6s$ .

## **6 Quantification of basin amplification: Simulation modelling**

### **6.1 Summary**

We have performed ground motion simulations of 19 major events in the Wellington (Figure 6a) using a model for the latest understanding of the sedimentary basin. This work leverages the ground motion simulation validation studies of Lee and Bradley [2019] with specific application to the Wellington region. Readers interested in a greater understanding of the simulation method should consult that reference.

## 6.2 Wellington velocity model

Through a synthesis of prior work from Semmens et al. (2011) [in Wellington CBD] and Boon et al. (2011) [in Lower Hutt], as well as geologic cross-sections, we developed a surface over the Wellington region of sedimentary basin depth, as shown in Figure 13. Since the development of this model, the model of Kaiser et al. [2019] has become available, and we are continuing to refine our modelling with this update as part of the National Seismic Hazard Model update.

## 6.3 Spectral ratios from simulations

Similar to the empirical analysis results presented in the prior section, it is useful to examine the ratio of ground motion intensity with reference to that of rock site. Figure 14 provides an illustration of typical analysis results in the form of ground motion amplification in the Wellington CBD and Lower Hutt sedimentary basins relative to nearby rock outcrop ground motion levels (POTS and PTOS stations, respectively) for the considered events. In Wellington (Figure 14a) it is evident that there is significant amplifications in Thorndon, which increases with distance from the basin edge. There are also amplification effects in the Te Aro basin, but these are more localised in nature, and don't extend significantly 'inland' toward Newtown. There is also muted amplification in the Evan's/Lyall Bay region. All of these trends are qualitatively consistent with observed ground motions in these areas. Figure 14b illustrates that the basin amplification in Lower Hutt is largest at the Petone waterfront and generally decreases proceeding up valley - consistent with observations [Bradley et al., 2017c].

## 6.4 Sensitivity study

While the analyses presented above are qualitatively consistent with observations (in a spatial sense), we identified that soil-to-rock amplifications at long vibration periods were lower in the simulations than in observations. We hypothesised that this could be the result of: (a) the use of a minimum velocity of  $V_s = 500$  m/s in the simulations; and/or (2) the assumption that the rock beneath the sedimentary basin is immediately crystalline, rather than having an appreciable depth of weathering.

In order to examine the sensitivity of the simulations to these assumptions, we have conducted simulations which reduced the minimum shear wave velocity from 500 down to 300 m/s, and also considered two different velocity models, v2.03 (sediments over crystalline basement), and v2.04 (a weathered basement layer added below the sediments).

### 6.4.1 3D simulations: Minimum $V_s = 300$ m/s sensitivity study

The logic of this sensitivity study was that using a minimum  $V_s = 300$ m/s this would shift the fundamental period to smaller values, which will improve compatibility with observations.

Initially, we ran into numerical stability issues in these calculations as a result of sharp contrasts between velocities (soil to rock) and large ratios of P- and S-wave velocities. These numerical issues have been resolved.

The numerical results observed with the lower minimum velocity had marginal difference from the baseline analysis case, and hence our reason for subsequently considering the use of a weathered basement layer.

#### 6.4.2 3D simulations: Weathered basement sensitivity study

In order to consider the effects of weathered basement rock, and unsymmetric fracturing on the hanging and footwall sides of the Wellington Fault zone, we considered two versions of the Wellington velocity model, shown in Figure 15. The logic for considering weathered basement was that the depth and velocities of the shallow sedimentary material could explain the amplifications in the  $T 1s$  vibration period range, but not that observed at longer periods.

Figure 16 and 17 provide an example of the site amplification at basin locations in Wellington and Lower Hutt, respectively, and their sensitivity to the assumption of weathered rock. While the level of amplification varies by location, generally speaking it can be seen that the weathered rock assumption leads to increased amplification at vibration periods  $T > 0.5s$  (as expected). The simplicity of the shape of the Lower Hutt basin (largely a 2D geometry) makes the trends simple, whereas the complex shape of the Wellington basin makes the effects more complex.

### 6.5 2D simulations

To provide a complement to 3D simulations we also examined a 2D plane strain model, as discussed in the attached paper (McGann et al. 2020). The same general conclusions for the 3D analyses were confirmed with these 2D analysis, and help provide us confidence in proceeding with the more extensible 3D analyses.

### 6.6 Summary insights from preliminary simulation work

Our results indicate that we are able to capture the key phenomena leading to the ‘amplification bump’ in the response spectra in the  $T = 1 - 5s$  vibration period range that is pervasive in the 2016 Kaikura, and other, past earthquakes. Despite this, sensitivity studies indicate that the size of this amplification is significantly affected by the near surface shear wave velocities at the site (summarised by  $V_{s30}$ ) and also the extent to which lateral variations in stiffness/velocity exist across the Wellington fault zone (as a result of unsymmetric rock fracturing).

These sensitivity studies strongly point to the need to: (i) better constrain the near-surface soil properties at the strong motion station; and (ii) improve the representation of the basement rock characterisation. In light of this work, external (to EQC) funding has been secured to undertake shallow characterisation of the GeoNet strong motion stations in the region. As yet, there are no immediate plans to undertake deep investigations that would shed light on the basement rock characterisation, so this will remain a significant unknown that requires further scientific understanding.

## 7 Ongoing work required

This biennial grant was funded soon after the 2016 Kaikura earthquake with an immediate need for rapid results to inform post-earthquake decision making around the evolution of the hazard understanding in Wellington. In parallel with receiving this EQC funding it was expected that MBIE funding (based on advanced discussions following the Statistics House Commission of Enquiry) would have been provided to complement the modest EQC Biennial funding available - that MBIE funding never eventuated. As a result, this

project was left with lofty ambitious, but insufficient resources to achieve all of them. Recognising this, EQC did provide some additional investment in this topic through the project "Wellington Basin - Immediate Research Outcomes" in order to accelerate the progress, and that is reflected in the extent of the work reported here.

It is broadly recognised that there remains much to do in order to understand the nature and extent of the effects of the sedimentary basin in the seismic hazard of Wellington, as well as the lessons it can provide for other regions of New Zealand and internationally. The commencement of the (MBIE-funded) National Seismic Hazard Model project from 2020-2022 provides a significant increase in resources that are available to address this problem, with a specific objective on the Wellington Basin. The investigators in this project are involved in that project, along with numerous others, and we anticipate that appreciable advances will be able to be made with this additional resourcing and the accumulation of knowledge through building on the research in this report.

## 8 Acknowledgements

The early support of EQC was instrumental to allow this work to progress consistently since the 2016 Kaikura earthquake, addressing a critical topic that has not easily funded due to the uncomfortable implications that it has for the increased seismic hazard in the Wellington region. This project was also partially supported from a Royal Society of New Zealand Rutherford Discovery Fellowship, and QuakeCoRE: The New Zealand Centre for Earthquake Resilience.

## References

- Sanjay Singh Bora, Frank Scherbaum, Nicolas Kuehn, and Peter Stafford. On the Relationship between Fourier and Response Spectra: Implications for the Adjustment of Empirical GroundMotion Prediction Equations (GMPEs). *Bulletin of the Seismological Society of America*, 106(3):1235–1253, June 2016. doi: 10.1785/0120150129. URL <http://bssa.geoscienceworld.org/content/ssabull/106/3/1235.full.pdf>.
- B.A. Bradley, L.M. Wotherspoon, and A.E. Kaiser. Ground motion and site effect observations in the wellington region from the 2016 mw7.8 kaikoura, new zealand earthquake. *Bulletin of the New Zealand Society for Earthquake Engineering*, 50(2):94–105, 2017a.
- Brendon A. Bradley. A new zealand-specific pseudospectral acceleration ground-motion prediction equation for active shallow crustal earthquakes based on foreign models. *Bulletin of the Seismological Society of America*, 103(3):1801–1822, 2013. doi: 10.1785/0120120021. URL <http://www.bssaonline.org/content/103/3/1801.abstract>.
- Brendon A. Bradley, Hoby N. T. Razafindrakoto, and Viktor Polak. Groundmotion observations from the 14 november 2016 mw7.8 kaikoura, new zealand, earthquake and insights from broadband simulations. *Seismological Research Letters*, 88(3):740–756, 2017b. doi: 10.1785/0220160225.
- Brendon A. Bradley, L.M. Wotherspoon, and A.E. Kaiser. Ground motion and site effect observations in the Wellington region from the 2016 Mw7.8 Kaikoura, New Zealand earthquake. *Bulletin of the New Zealand Society for Earthquake Engineering*, 50(2):94–105, 2017c.

*Society of America*, 108(3B):1722–1735, March 2018. ISSN 0037-1106. doi: 10.1785/0120170286.

- A. Kaiser, C. Van Houtte, N. Perrin, L. Wotherspoon, and G. McVerry. Site characterisation of geonet stations for the new zealand strong motion database. *Bulletin of the New Zealand Society for Earthquake Engineering*, 50(1):39–49, 2017.
- A.E. Kaiser, M.P. Hill, L.M. Wotherspoon, S. Bourguignon, Z. Bruce, R. Morgenstern, and S Gaillini. Updated 3D basin model and NZS1170.5 subsoil class and site period maps for the Wellington CBD: Project 2017-GNS-03-NHRP, May 2019.
- R.L. Lee and B.A. Bradley. Progress toward New Zealand-wide hybrid broadband ground motion simulation validation. In *2019 Pacific Conference on Earthquake Engineering*, page 8, Auckland, New Zealand, 2019.
- S. Semmens, N.D. Perrin, G.D. Dellow, and R. Van Dissen. NZS1170.5:2004 site subsoil classification of Wellington City. *9th Pacific Conference on Earthquake Engineering*, 2011.
- C. Van Houtte, S. Bannister, C. Holden, S. Bourguignon, and G. McVerry. The new zealand strong motion database. *Bulletin of the New Zealand Society for Earthquake Engineering*, 50(1):1–20, 2017.
- Joseph Vantassel, Brady Cox, Liam Wotherspoon, and Andrew Stolte. Mapping depth to bedrock, shear stiffness, and fundamental site period at CentrePort, wellington, using surfacewave methods: Implications for local seismic site amplification. 108(3):1709–1721, 2018. ISSN 0037-1106. doi: 10.1785/0120170287. URL <http://dx.doi.org/10.1785/0120170287>.

(a) PIPS

(b) WEMS

(c) TFSS

(d) VUWS

(e) FKPS

(f) TEPS

Figure 8: Spectral amplification observed <sup>20</sup> at the six considered strong motion stations relative to the POTS reference site and in comparison to the NZS1170.5 site class D amplification relative to site class B. NOTE: Adjust all y-axes to have constant max values along lines. GRL Report (and for Kiteh et al.) refers to this. Data plotted are

Figure 9: Mean site amplification factors from the reference site approach as compared to the empirically-predicted site amplification.

Figure 10: Ratio of the site amplification factors and the empirically-predicted site amplification. The mean of the three sites is denoted as the ‘model’, and the principal result from Method 1.

(a) Bias

(b) Site-to-site term

(c) Systematic site effect

Figure 11: Results of mixed-effects analysis at strong motion stations of relevance, and the smoothed model for site correction via Method 2.

Figure 12: Comparison of the site amplification factors from the two methods, and the proposed amplification function to be applied to adjust the ergodic PSHA results

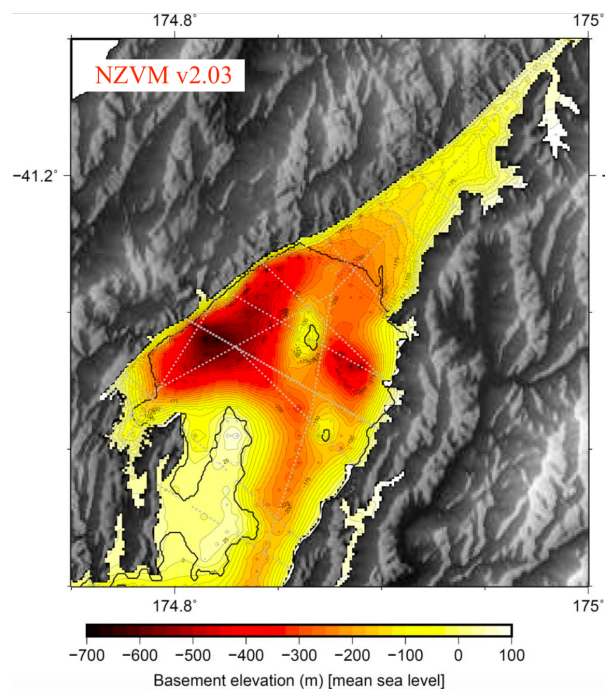
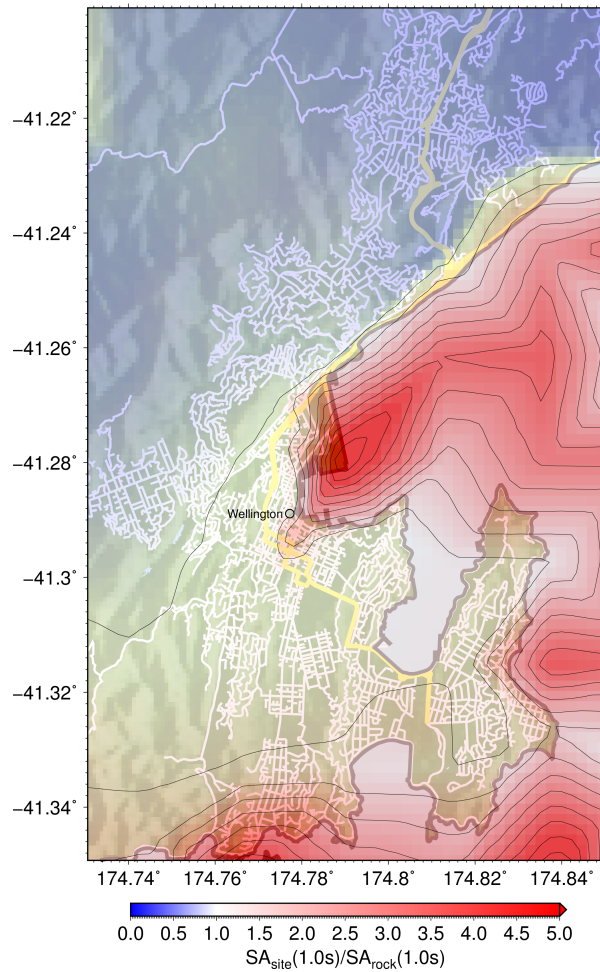


Figure 13: Illustration of modelled Wellington Basin depth based on Semmens et al. (2011), Boon et al. (2011), and geologic cross-sections.

Response spectral amplification



Response spectral amplification

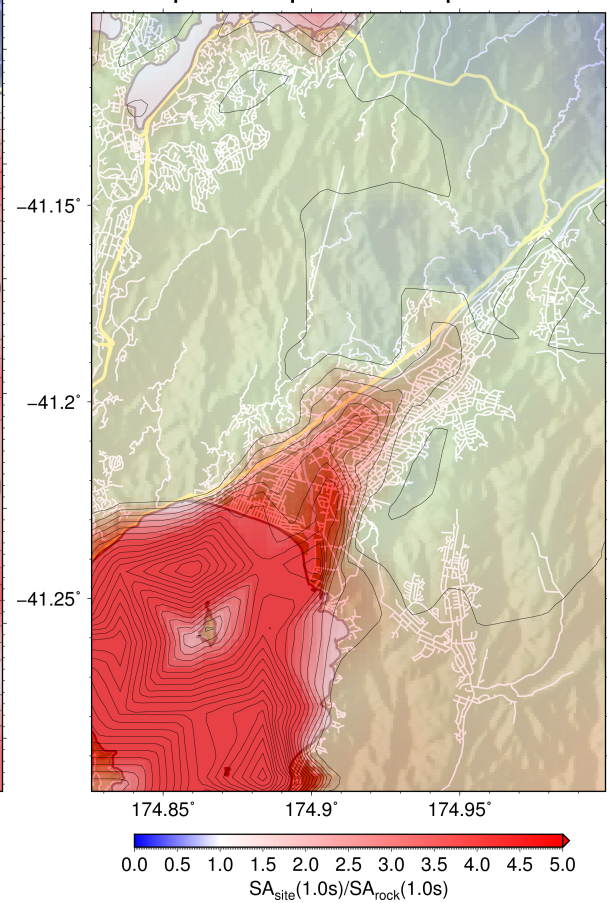


Figure 14: Illustration of site amplification in the form of  $SA(1.0s)$  response spectral ratios in Wellington city and Lower Hutt.

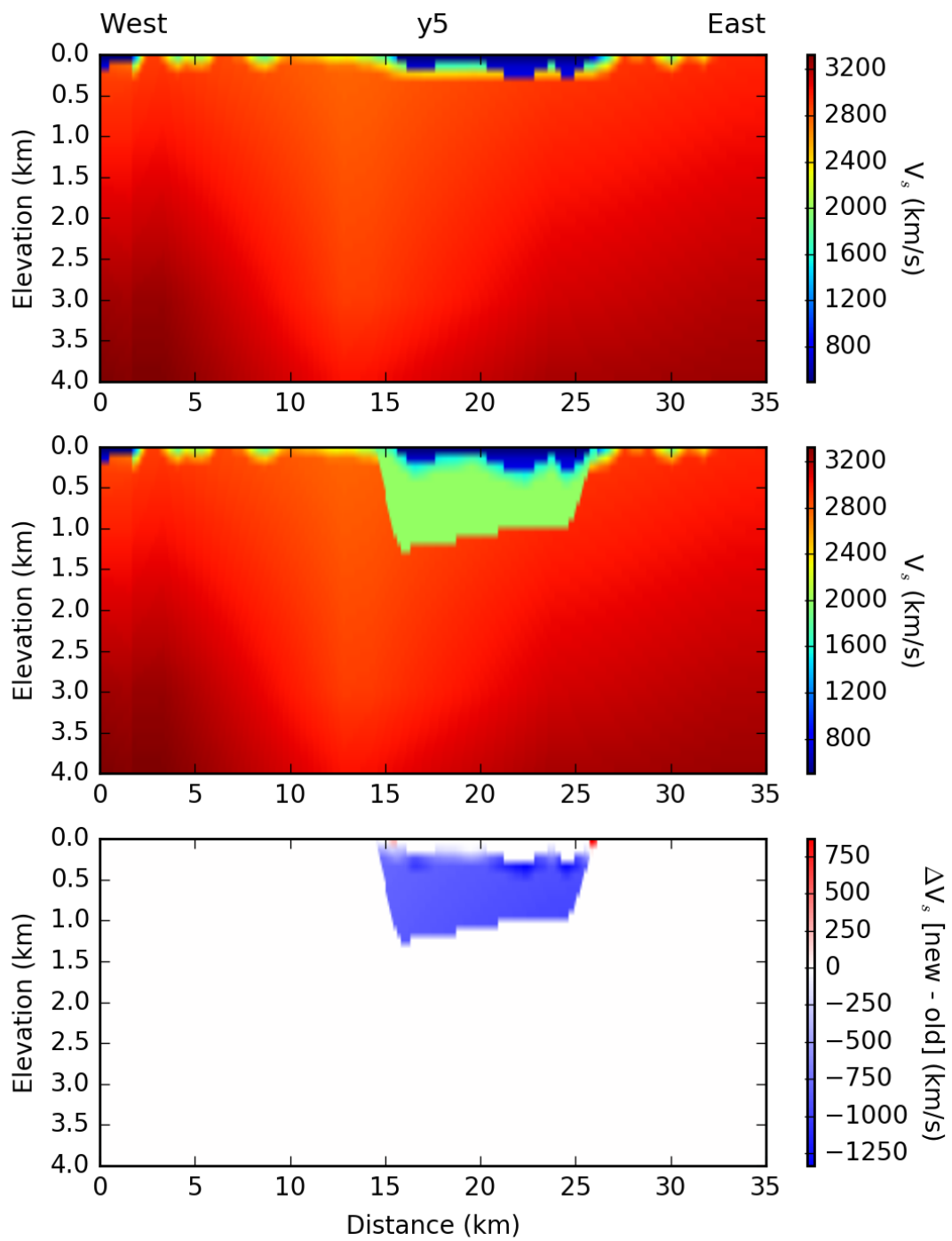


Figure 15: Velocity model cross-section (West to East across the Wellington CBD) illustrating modelled Wellington with and without weathered basement: (a) without; (b) with; (c) difference of (a) and (b).

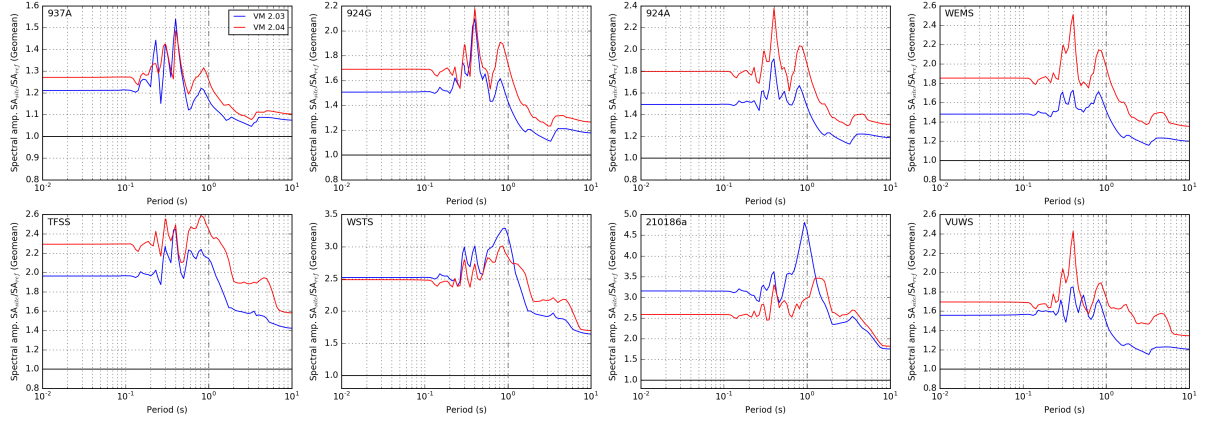


Figure 16: Example comparisons of spectral amplifications at Wellington basin sites (as a ratio to nearby outcropping rock) based on the inclusion of the weathered basement rock.

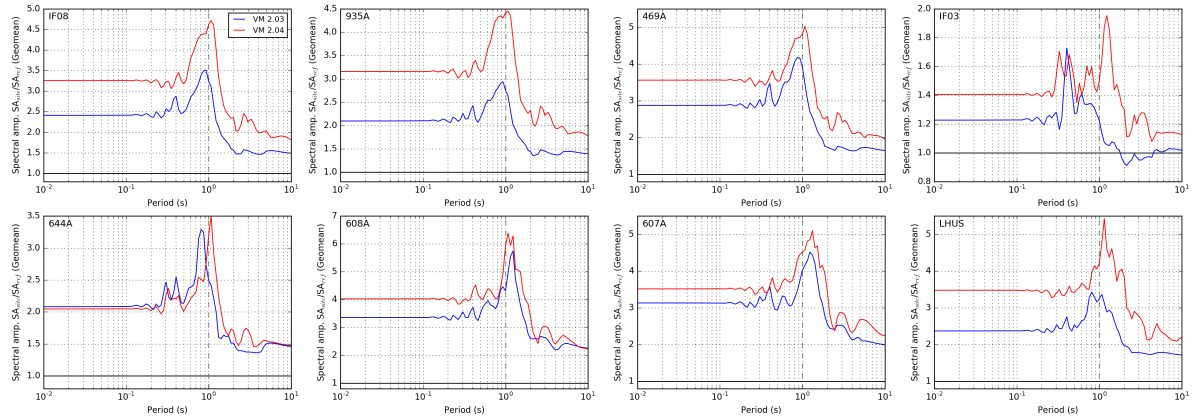


Figure 17: Example comparisons of spectral amplifications at Lower Hutt basin sites (as a ratio to nearby outcropping rock) based on the inclusion of the weathered basement rock.